



Energy transfer assisted frequency upconversion in Ho 3+ doped fluoroindate glass

N. Rakov, G. S. Maciel, Cid B. de Araújo, and Y. Messaddeq

Citation: [Journal of Applied Physics](#) **91**, 1272 (2002); doi: 10.1063/1.1430889

View online: <http://dx.doi.org/10.1063/1.1430889>

View Table of Contents: <http://scitation.aip.org/content/aip/journal/jap/91/3?ver=pdfcov>

Published by the [AIP Publishing](#)



Re-register for Table of Content Alerts

Create a profile.



Sign up today!



Energy transfer assisted frequency upconversion in Ho^{3+} doped fluorindate glass

N. Rakov, G. S. Maciel, and Cid B. de Araújo^{a)}

Departamento de Física, Universidade Federal de Pernambuco, 50670-901 Recife, PE, Brazil

Y. Messaddeq

Departamento de Química, Universidade do Estado de São Paulo, 14800-900 Araraquara, SP, Brazil

(Received 21 August 2001; accepted for publication 6 November 2001)

Experimental results are reported which show a strong evidence of energy transfer between Ho^{3+} ions in a fluorindate glass excited by a pulsed laser operating at 640 nm. We identified the origin of the blue and green upconverted fluorescence observed as being due to a Ho^{3+} - Ho^{3+} pair interaction process. The dynamics of the fluorescence revealed the pathways involved in the energy transfer assisted upconversion process. © 2002 American Institute of Physics.

[DOI: 10.1063/1.1430889]

I. INTRODUCTION

The luminescence of rare earth (RE) ions in different host materials has been extensively studied. Although there are a large number of reports on this subject,¹⁻³ in recent years a renewed interest in the investigation of frequency upconversion (UPC) processes in RE doped materials, motivated by the possibility of using the UPC phenomenon to develop efficient sensors, quantum counters, and lasers operating in the blue-green spectral region, has been observed.

One of the most studied RE ions has been holmium (Ho^{3+}). The optical properties of Ho^{3+} in crystalline and amorphous environments have been studied, aimed at the operation of UPC lasers to be used in, for example, odonthological treatment.⁴ Blue-green UPC luminescence owing to $4f-4f$ transitions of Ho^{3+} has been observed upon visible and infrared excitation with efficiencies that are highly dependent on the host matrix⁵⁻⁸ demonstrating the importance of studying UPC processes in different materials.

Among the materials being investigated to date, RE doped fluorindate glasses (FIGs) emerged as efficient upconverters.⁹⁻¹⁵ These glasses present phonons of low energy ($\leq 507 \text{ cm}^{-1}$) that inhibits nonradiative relaxation channels in favor of radiative channels (luminescence). Besides, FIGs present great resistance to atmospheric moisture and good mechanical stability. It is also possible to incorporate large concentrations of RE ions inside the matrix (up to 10 mol %) and as a consequence different energy transfer mechanisms have been observed in FIGs doped with praseodymium,⁹ erbium,¹⁰⁻¹² neodymium,¹³ codoped with ytterbium and praseodymium,¹⁴ and codoped with ytterbium and holmium.¹⁵

In this article we investigate possible UPC pathways in Ho^{3+} doped FIG using nanosecond excitation at 640 nm. Green and blue anti-Stokes emissions, owing to energy transfer mechanisms, were observed whose time evolution occurs

in different time scales. The analysis of the results allowed us to identify the energy transfer pathways that contribute to the UPC emissions.

II. EXPERIMENT

The samples used have the following compositions in mol %: $38\text{InF}_3-20\text{ZnF}_2-20\text{SrF}_2-(16-x)\text{BaF}_2-2\text{NaF}-4\text{GaF}_3-x\text{HoF}_3$, where $x=0.5, 1.0$ and 2.0 . The glass synthesis was made using standard proanalysis oxides and fluorides as starting materials. The fluoride powders used to prepare the desired compositions were mixed together and heat treated first at 700°C for melting and then 800°C for refining. The melt was finally poured between two preheated brass plates to allow the preparation of samples of different thicknesses. Fining, casting, and annealing were carried out in a way similar to standard fluoride glasses under a dry argon atmosphere. Nonhygroscopic samples are obtained with very good optical quality.

The UPC measurements were performed using a dye laser pumped by the second harmonic of a Q -switched Nd:YAG laser (532 nm, 15 ns, 5 Hz). The dye laser beam was focused on the sample using a focal length lens of 2.5 cm. The fluorescence signal, dispersed by a 0.25 m spectrometer, was detected by a GaAs photomultiplier tube and sent to a digital oscilloscope. The average of many successive scans was recorded in a computer. All measurements were performed at room temperature.

III. RESULTS AND DISCUSSION

The linear absorption spectrum of Ho^{3+} doped FIG (with $x=2$) is shown in Fig. 1. No changes were observed in the line shape or in the peak positions associated with the various transitions for different Ho^{3+} concentrations.

The method of spectral-band intensity analysis¹⁶ was used to estimate the Judd-Ofelt parameters of our sample and the values found were $\Omega_2=1.37\times 10^{-20} \text{ cm}^2$, $\Omega_4=2.35\times 10^{-20} \text{ cm}^2$, and $\Omega_6=2.22\times 10^{-20} \text{ cm}^2$.

^{a)} Author to whom correspondence should be addressed; electronic mail: cid@df.ufpe.br

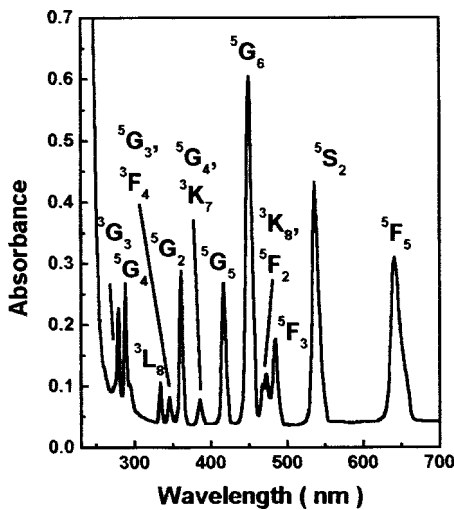


FIG. 1. Linear absorption spectrum of the Ho³⁺ doped fluoroindate glass (sample with $x=2$; thickness: 1.5 mm).

The forced electric dipole transition probability (radiative emission rate) between states aJ and bJ' was calculated using the equation^{17,18}

$$A(a, J; b J') = \frac{64\pi^4 \nu^3 e^2}{3hc^3(2J+1)} \frac{n(n^2+2)^2}{9} \times \sum_{i=2,4,6} \Omega_i |\langle aJ \| U^{(i)} \| bJ' \rangle|^2, \quad (1)$$

where n is the index of refraction of the material, ν is the photon frequency, J is the total angular momentum, e is the electronic charge, h is the Planck's constant, and c is the speed of light in vacuum. The term inside the squared modulus is the reduced matrix element.¹⁹ From the values obtained, it is possible to calculate the radiative lifetime τ_r of an excited state i which is given by

$$\frac{1}{(\tau_r)_i} = \sum_j A(i, j). \quad (2)$$

We also used the "energy gap law"²⁰ to estimate the nonradiative emission rate A_{nr} in our samples. The values of A , τ_r , and A_{nr} for the levels involved in the energy transfer processes studied here are given in Table I.

The observed UPC spectrum of Ho³⁺ doped FIG is shown in Fig. 2 for excitation at 640 nm, in resonance with the transition $^5I_8 \rightarrow ^5F_5$. Figure 2(a) shows two bands centered at ~ 550 and ~ 490 nm corresponding to transitions $^5S_2 \rightarrow ^5I_8$ and $^5F_3 \rightarrow ^5I_8$, respectively, while Fig. 2(b) shows

TABLE I. Spontaneous emission probabilities of the main Ho³⁺ excited states of interest in fluoroindate glass.

Energy level	A_r (s ⁻¹)	τ_r (ms)	A_{nr} (s ⁻¹)
5F_5	2.15×10^3	0.5	3×10^4
5S_2	2.54×10^3	0.4	1×10^3
5F_3	5.47×10^3	0.2	2×10^5
$^5G_4, ^3K_7$	4.67×10^3	0.2	6×10^5
5G_5	5.50×10^3	0.2	6×10^5

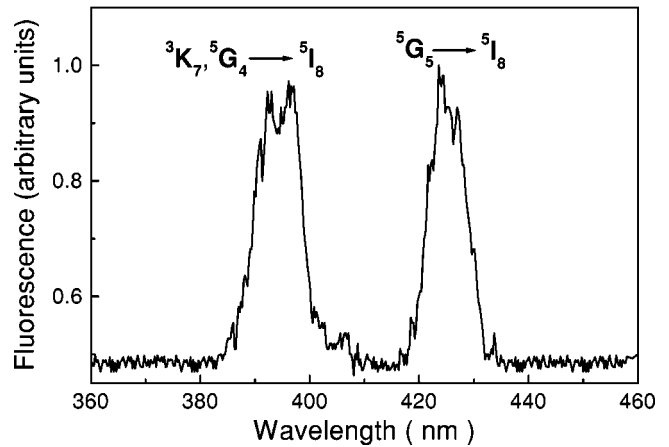
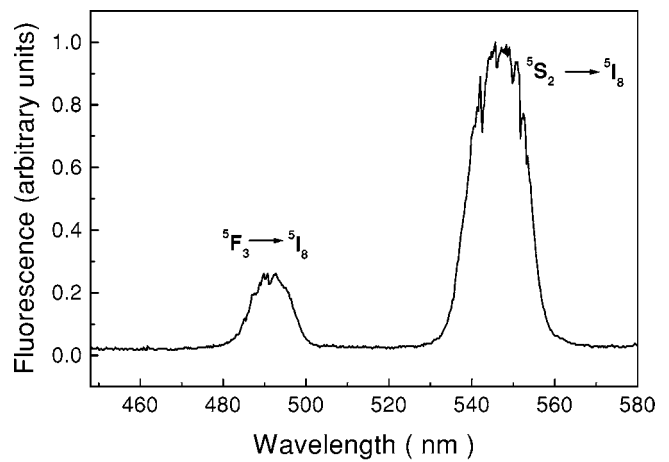


FIG. 2. Fluorescence upconversion emission (sample with $x=2$): (a) blue-green region and (b) violet-blue region.

bands centered at ~ 395 and ~ 425 nm corresponding to transitions $(^3K_7, ^5G_4) \rightarrow ^5I_8$ and $^5G_5 \rightarrow ^5I_8$, respectively. The intensity of the bands shown in Fig. 2(b) are 2 orders of magnitude weaker than those shown in Fig. 2(a).

The dynamics of the UPC luminescence at ~ 550 nm (green) and ~ 490 nm (blue) are illustrated in Figs. 3(a) and 3(b), respectively. Note that the temporal evolution of the green luminescence signals present a rise time between 3.2 and 4.2 μ s, and a decay time that changes more than 50% (116–48 μ s) for the range of Ho³⁺ concentrations investigated here. The blue luminescence presents a rise time that is shorter compared with the green signal, and it shows a double-exponential decay. The longer decay time component of the blue emission (22–18 μ s) is also dependent on the Ho³⁺ concentration. The results are summarized in Table II. The dependence of the UPC signal as a function of pump intensity and Ho³⁺ concentration were also investigated. A quadratic dependence was observed in both experiments indicating that two laser photons are absorbed to originate each UPC photon and a pair of Ho³⁺ ions are involved in the process that leads to UPC emission.

The signals observed in the region from ~ 380 to ~ 440 nm are very weak and it was not possible to analyze their temporal behavior. It is important to note that these emissions have not been observed in other glass hosts⁶ probably because their intensities were too small in those systems.

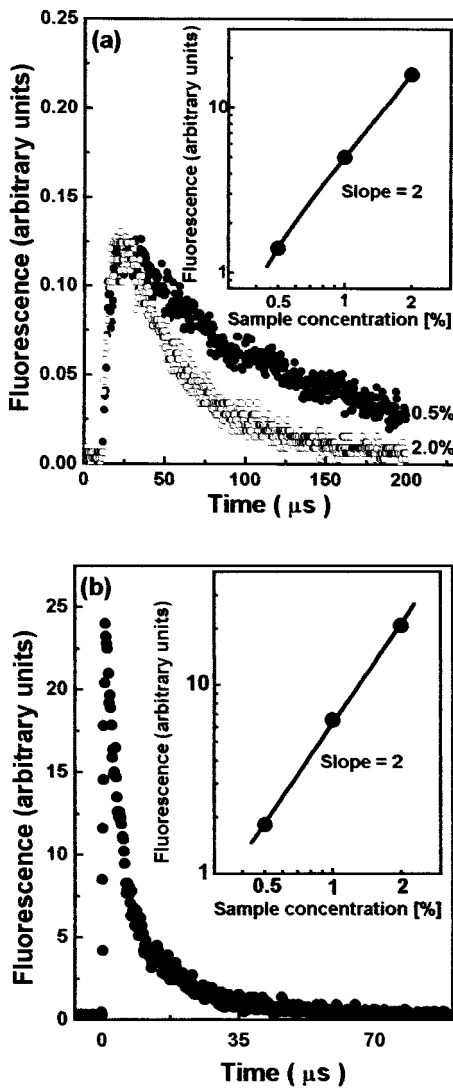


FIG. 3. Temporal behavior of the upconverted fluorescence of Ho^{3+} doped FIG under pulsed excitation at 640 nm. (a) ${}^5S_2 \rightarrow {}^5I_8$ green fluorescence for two concentrations. (Inset) Dependence of the green fluorescence intensity as a function of the sample concentration. (b) Time evolution of ${}^5F_3 \rightarrow {}^5I_8$ blue fluorescence. (Inset) Dependence of the blue fluorescence intensity as a function of the sample concentration.

In general, two mechanisms may lead to UPC emission: excited state absorption (ESA) and energy transfer (ET). The efficiency of an ESA process is determined mainly by a resonance condition of the excitation laser with an excited state transition. The ET process, on the other hand, may arise from

TABLE II. Dynamics of the upconversion luminescence of Ho^{3+} doped fluoroindate glasses. The excitation pulse is a nanosecond laser emitting at 640 nm. Estimated data error: 5%.

$[\text{Ho}^{3+}]$ (mol %)	0.5	1	2
Rise time@548 nm	3.6 μs	4.2 μs	3.2 μs
Decay time@548 nm	116 μs	78 μs	48 μs
Rise time@490 nm	0.4 μs	0.4 μs	0.4 μs
Decay time(1)@490 nm	3 μs	3 μs	3 μs
Decay time(2)@490 nm	22 μs	20 μs	18 μs

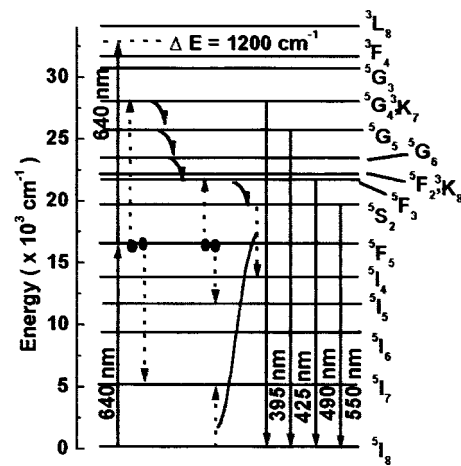


FIG. 4. Ho^{3+} energy levels relevant to the frequency upconversion processes studied and the possible excitation pathways including cross-relaxation processes involved.

both electric multipole and exchange interactions among neighboring ions, and its strength is strongly dependent on the ion-ion separation.²¹

Figure 4 shows the energy level diagram of Ho^{3+} and the main pathways responsible for the upconversion processes. Considering our pumping scheme and the energy levels of Ho^{3+} ions, different processes could be considered to understand the generation of the UPC emissions observed: (i) ESA via sequential two-photon absorption through ${}^5I_8 \rightarrow {}^5F_5$ followed by ${}^5F_5 \rightarrow {}^3F_4$ transition. However, in the present case, this process is not important because the laser frequency is off resonance with transition ${}^5F_5 \rightarrow {}^3F_4$ by $\sim 1200 \text{ cm}^{-1}$. (ii) Another way to populate high lying energy levels could be via resonant ESA through transition ${}^5I_4 \rightarrow {}^5G_3$. Nevertheless, this channel is irrelevant for nanosecond excitation because the relaxation from level 5F_5 to level 5I_4 is slow compared with the laser pulse duration (the lifetime of level 5F_5 is $\sim 47 \mu\text{s}$).²² (iii) Another possibility is ET due to the interaction between two ions at level 5F_5 which is directly excited by laser photons at 640 nm. The lifetime of level 5F_5 is large enough to allow significant ET between excited ions and two possible channels may populate level 5F_3 via ET.⁶ One channel is an *indirect* ET assisted UPC (ETAU) via ${}^5F_5 + {}^5F_5 \rightarrow {}^5I_7 + ({}^3K_7, {}^5G_4)$ with subsequent population decay to level 5F_3 via multiphonon emission from levels 5G_4 and 3K_7 . The other channel is related to a *direct* ETAU via ${}^5F_5 + {}^5F_5 \rightarrow {}^5I_5 + {}^5F_3$. Process (iii) is the most probable to occur in the present case, as evidenced in the inset of Fig. 3, which shows a square dependence of the UPC signal with Ho^{3+} concentration, indicating that pair interaction is the relevant process.

Using a rate equations approach to describe process (iii), it is possible to estimate the ET rates from level 5F_5 to level 5F_3 considering the following equations:

$$dN_d/dt = -2\gamma_1 N_d - (W_{12} + W_{13})N_d, \quad (3)$$

$$dn_2/dt = -\gamma_2 n_2 + \gamma_{32} n_3 + W_{12} N_d, \quad (4)$$

$$dn_3/dt = -\gamma_3 n_3 + W_{13} N_d. \quad (5)$$

TABLE III. Values of the energy transfer rates responsible for the blue and green upconversion.

[Ho ³⁺] (mol %)	0.5	1	2
$W_{12} + W_{13}$ (s ⁻¹)	3×10^3	7×10^3	13×10^3
W_R (s ⁻¹)	6×10^3	10×10^3	18×10^3

Here, N_d represents the population density belonging to a pair of excited ions at level 5F_5 [the factor of 2 in Eq. (3) arises because an excited pair is annihilated as soon as one of the ions de-excites], $(\gamma_1)^{-1}$ is the lifetime of level 5F_5 , and n_2 and n_3 stand for the population densities of level 5F_3 and level $({}^3K_7, {}^5G_4)$, respectively. The parameters $(\gamma_2)^{-1}$ and $(\gamma_3)^{-1}$ are the lifetimes of level 5F_3 and level $({}^3K_7, {}^5G_4)$, respectively. γ_{32} is the multistep nonradiative decay rate from level $({}^3K_7, {}^5G_4)$ to level 5F_3 , and W_{ij} ($i, j = 1, 2, 3$) are cross-relaxation rates. The dynamics of the population at level 5F_3 is found by solving the system of Eqs. (3)–(5) and the solution is given by

$$n_2(t) = Ae^{-(2\gamma_1 + W_{12} + W_{13})t} - Be^{-\gamma_3 t} + Ce^{-\gamma_2 t}. \quad (6)$$

The fluorescence intensity at ~ 490 nm is proportional to $n_2(t)$ and comparing Eq. (6) with the data shown in Table II we associate γ_2 to the short decay time component, that is independent of Ho³⁺ concentration, and therefore it is related to level 5F_3 lifetime (estimated ~ 5 μ s from Table I). The value of $(\gamma_3)^{-1}$ is dominated by $(\gamma_{32})^{-1} \sim 0.6$ μ s, while the lifetime of 5F_5 is $(\gamma_1)^{-1} \sim 47$ μ s.²² Therefore $(\gamma_3)^{-1}$ is associated with the rise time of the blue luminescence while $(2\gamma_1 + W_{12} + W_{13})^{-1}$ is associated with the longer decay time. The cross-relaxation rates found for our samples are shown in Table III. The fact that the measured rise time (0.4 μ s) was shorter than the estimated multistep multiphonon emission rates from level $({}^3K_7, {}^5G_4)$ may account for the fact that the signal centered at ~ 490 nm has a contribution from excited pairs decaying coherently (simultaneously) to lower-lying energy levels on a faster time scale than those pairs decaying incoherently.

To understand the behavior of the emission at ~ 550 nm, we assume that the population at level 5S_2 is loaded via level 5F_3 because the rise time of the green fluorescence has the same order of magnitude as the lifetime of 5F_3 , that is dominated by the nonradiative relaxation ${}^5F_3 \rightarrow {}^5S_2$ (2×10^5 s⁻¹). We note that the green fluorescence decay time is dependent on the Ho³⁺ concentration as indicated in Table II. The cross-relaxation channel that depopulates level 5S_2 (${}^5S_2 + {}^5I_8 \rightarrow {}^5I_4 + {}^5I_7$) is efficient only after the cross-relaxation processes that lead to the blue luminescence takes place (see Fig. 4).⁶ Again, the rate equations approach is used to estimate the cross-relaxation rates from level 5S_2 through the following equations:

$$dn_1'/dt = -\gamma_1' n_1', \quad (7)$$

$$dn_2'/dt = \gamma_1' n_1' - (\gamma_2' + W_R) n_2'. \quad (8)$$

Here, 1 corresponds to level 5F_3 of the excited ion of the pair and 2 is associated with level 5S_2 . The parameter γ_1' (γ_2') is the decay rate of level 5F_3 (5S_2) and W_R is the cross-

relaxation rate. The ground state population was assumed to be nondepleted and thus the solution of the rate equations system yielded a simple equation that governs the dynamics of the population at level 5S_2 :

$$n_2'(t) = Ae^{-\gamma_1' t} - Be^{-(\gamma_2' + W_R)t}. \quad (9)$$

In Eq. (9), $(\gamma_1')^{-1}$ is the lifetime of level 5F_3 and $(\gamma_2' + W_R)^{-1}$ corresponds to the quenched lifetime of level 5S_2 . As the values of γ_1' and γ_2' are known, it is straightforward to find W_R from the data of Tables I and II and the values found for W_R are shown in Table III.

IV. CONCLUSIONS

In conclusion, we observed that ET is the mechanism responsible for the red-to-blue-and-green frequency upconversion in Ho³⁺ doped FIG glass under nanosecond laser excitation. Two ET assisted upconversion channels (ETAU) between Ho³⁺ ions were identified: one is the *indirect* ETAU ${}^5F_5 + {}^5F_5 \rightarrow {}^5I_7 + ({}^5G_4, {}^3K_7)$ followed by multiphonon relaxation $({}^3K_7, {}^5G_4) \rightarrow {}^5F_3$ and the other channel is the *direct* ETAU ${}^5F_5 + {}^5F_5 \rightarrow {}^5I_5 + {}^5F_3$. The results were described using rate equations for the level populations, which include the important contributions of cross relaxations. From the experimental data the values of the ET parameters responsible for blue and green fluorescence were obtained.

ACKNOWLEDGMENTS

This work was supported by the Brazilian agencies Conselho Nacional de Desenvolvimento Científico e Tecnológico (CNPq), Fundação Coordenação de Aperfeiçoamento de Pessoal de Nível Superior (CAPES), and Fundação de Amparo à Ciência e Tecnologia (FACEPE).

¹ See, for example, *Rare-Earth Doped Fiber Lasers and Amplifiers*, edited by M. J. Digonnet (Marcel Dekker, New York, 1993), and references therein.

² J. X. Meng, K. F. Li, and J. Yuan, Chem. Phys. Lett. **332**, 313 (2000).

³ S. Bhattacharyya, L. R. Sousa, and S. Ghosh, Chem. Phys. Lett. **297**, 154 (1998).

⁴ T. G. Barton, H. J. Foth, M. Christ, and K. Hörmann, Appl. Opt. **36**, 32 (1997).

⁵ S. Kück and I. Sokólska, Chem. Phys. Lett. **325**, 257 (2000).

⁶ M. Malinowski, R. Piramidowicz, Z. Frukacz, G. Chadeyron, R. Mahiou, and M. F. Joubert, Opt. Mater. **12**, 409 (1999).

⁷ B. R. Reddy, S. Nash-Stevenson, and P. Venkateswarlu, J. Opt. Soc. Am. B **11**, 923 (1994).

⁸ P. Müller, M. Wermuth, and H. U. Güdel, Chem. Phys. Lett. **290**, 105 (1998).

⁹ L. E. E. de Araújo, A. S. L. Gomes, C. B. de Araújo, Y. Messaddeq, A. Florez, and M. A. Aegerter, Phys. Rev. B **50**, 16219 (1994).

¹⁰ G. S. Maciel, C. B. de Araújo, Y. Messaddeq, and M. A. Aegerter, Phys. Rev. B **55**, 6335 (1997).

¹¹ G. S. Maciel, N. Rakov, C. B. de Araújo, and Y. Messaddeq, J. Opt. Soc. Am. B **16**, 1995 (1999).

¹² W. Lozano B., C. B. de Araújo, L. H. Acioli, and Y. Messaddeq, J. Appl. Phys. **84**, 2263 (1998).

¹³ G. S. Maciel, L. de S. Menezes, C. B. de Araújo, and Y. Messaddeq, J. Appl. Phys. **85**, 6782 (1999).

¹⁴ A. S. Oliveira, E. A. Gouveia, M. T. Araujo, A. S. Gouveia-Neto, C. B. de Araújo, and Y. Messaddeq, J. Appl. Phys. **87**, 4274 (2000).

¹⁵ R. Martín, V. D. Rodríguez, V. Lavín, and U. R. Rodríguez-Mendoza, J. Alloys Compd. **275**, 345 (1998).

- ¹⁶S. A. Payne, J. A. Caird, L. L. Chase, L. K. Smith, N. D. Nielsen, and W. F. Krupke, *J. Opt. Soc. Am. B* **8**, 726 (1991).
- ¹⁷B. R. Judd, *Phys. Rev.* **127**, 750 (1962).
- ¹⁸G. S. Ofelt, *J. Chem. Phys.* **37**, 511 (1962).
- ¹⁹W. T. Carnall, H. Crosswhite, and H. M. Crosswhite, Report, 1977.
- ²⁰K. Tanimura, M. D. Shinn, and W. Sibley, *Phys. Rev. B* **30**, 2429 (1984).
- ²¹D. L. Dexter, *J. Chem. Phys.* **21**, 836 (1953).
- ²²The Stokes-shifted emission at 653 nm (transition ${}^5F_5 \rightarrow {}^5I_8$) was used to evaluate the lifetime of level 5F_5 using the less concentrated sample ($x=0.5$) with low excitation power at 640 nm. The signal decay was fitted with a single-exponential curve yielding $\sim 47 \mu\text{s}$ of decay time.